Velocity prediction in high-gradient channels

Steven E. Yochum [a,*], Brian P. Bledsoe [a], Gabrielle C.L. David [b], Ellen Wohl [b]

[a] Colorado State University, Department of Civil and Environmental Engineering, Fort Collins, CO 80523, USA
[b] Colorado State University, Department of Geosciences, Fort Collins, CO 80523, USA

SUMMARY

In 15 mountain stream reaches containing instream wood, we characterized velocity and flow resistance at bankfull through low flows. These data were: (1) used to assess the accuracy of previously published velocity prediction techniques for high-gradient channels; and (2) were combined with field data from other studies to develop general methodologies for predicting velocity and flow resistance in alluvial and mixed alluvial-bedrock channels both with and without step-forming instream wood. Velocity and flow resistance were poorly predicted by variables characterizing grain size and relative grain submergence. Conversely, methods based on detrended standard deviation of bed elevations (σ_z) and relative bedform submergence (h/σ_z) explained up to 84% of the variance in the measured flow resistance coefficients and 97% of the variance in dimensionless velocity. With an average velocity of 0.44 m/s for the collected measurements, velocity was predicted with RMS (root mean square) error as low as 0.071 m/s (16% of average) when discharge and bedform geometry is known and 0.10 m/s (23%) when only bedform geometry is known. Additionally, an empirical relationship indicates $V/u^* = h/\sigma_z$, supporting previously-published laboratory findings using a field-based dataset in complex high-gradient channels. Interactions between instream wood and clasts result in substantially enhanced step heights and flow resistance. This compound effect defies description by grain size and relative grain submergence. However, σ_z and h/σ_z quantify variability due to both clasts in combination with wood and clasts alone, providing relatively accurate predictions for the tested dataset and indicating substantial predictive capabilities in channels where bedforms are the primary source of flow resistance.

Published by Elsevier B.V.

1. Introduction

Hydrologists and engineers are often called upon to predict velocity and flow resistance coefficients in stream channels. Velocity prediction is essential for channel analysis and design, geomorphic analyses, and ecological studies. Quantitative methods that accurately estimate velocity from simply-measured geometric characteristics are the most useful in application but are also the most elusive to obtain, especially for a full range of flows. In high-gradient channels (>~3%), limited guidance is available, with popular references for selecting Manning's n (Chow, 1959; Arcement and Schneider, 1989; Brunner, 2010), the most commonly-applied resistance coefficient, typically underestimating hydraulic resistance in high-gradient channels. The ramifications of this underestimation include substantially overestimated flow velocities, underestimated travel times, the miscategorization of flow regime, inaccurate design parameters for hydraulic structures, and instability in computational modeling.

Velocity is inversely proportional to flow resistance, with flow resistance increasing as discharge (stage) decreases (Limerinos, 1970; Bathurst, 1985; Lee and Ferguson, 2002; Wilcox and Wohl, 2006; Reid and Hickin, 2008; Ferguson, 2010). An assumption of constant resistance is inappropriate in high-gradient channels, since bedforms, instream wood and boulders are often similar in scale to flow depths. Generally, the variability in flow resistance and velocity by stage has been underemphasized by many engineers and hydrologists. Relative submergence, defined as the ratio of hydraulic radius (R) to a characteristic roughness element size such as grain size or a bedform characteristic, can assist in quantifying variability in flow resistance due to stage. Traditionally, the characteristic roughness is assumed to be a bed material size (D_{84}), though other measures of roughness may likely be more appropriate in channels with complex bedforms (Rouse, 1965; Kaufmann, 1987; Wohl et al., 1997; Aberle and Smart, 2003; Chin and Phillips, 2007; Kaufmann et al., 2008; Wohl and Merritt, 2008; David et al., 2010a,b). If reliable alternative measures of bedform influence can be identified, estimates of velocity and resistance throughout a range of discharges may be possible. Defining geometric characteristics of high-gradient channels that can be used to accurately predict average reach velocity is needed to provide

* Corresponding author. Present address: USDA Natural Resources Conservation Service, 2150 Centre Ave., Bldg. A, Ste. 116, Fort Collins, CO 80526, USA. Tel.: +1 970 295 5657.
E-mail address: steven.yochum@co.usda.gov (S.E. Yochum).

Nomenclature

A	flow area, computed as average of all reach sections (m^2)
a, b	surrogate explanatory variables
α	assumed acceptable probability of inappropriately rejecting the significance of an explanatory variable
δ	roughness layer thickness (m)
D_{50}, D_{84}, D_{90}	bed material size for which 50%, 84% and 90% of the material is finer (m)
D_c	roughness parameter for dimensionless velocity and discharge = σ_z, D_{84}
d_{res}	thalweg residual depth (m)
d_{th}	thalweg mean depth (m)
f	reach average Darcy-Weisbach roughness coefficient (dimensionless)
g	acceleration due to gravity ($9.81 m/s^2$)
h	flow depth (m)
$\bar{h}$	reach mean of cross-sectional average flow depth (m)
h_m	median maximum flow depth, from equally-spaced reach sections or thalweg longitudinal profile (m)
K_b	average sinuosity of channel wetted edge (dimensionless)
n	reach average Manning's roughness coefficient $(s/m^{1/3})$
N	number of points in sample
P_w	reach wetted perimeter, computed as average of all reach sections (m)
Q	discharge (m^3/s), measured via weir
Q^*	dimensionless discharge = $Q/(D_c\sqrt{gD_c^3})$
q	unit discharge (m^2/s) = Q/TW
$q*$	dimensionless unit discharge = $q/\sqrt{gD_c^3}$
$q**$	dimensionless unit discharge = $q/\sqrt{gSD_c^3}$

R	hydraulic radius = A/P_w
r	Pearson's correlation coefficient
R^2	coefficient of determination, fraction of explained variance
$R/\sigma_z, h_m/\sigma_z$	relative bedform submergence (dimensionless)
RMS error	root-mean-square error
S_f	friction slope (m/m)
S_o	bed slope (m/m)
TW	top width of the channel, computed as average of all reach sections (m)
u^*	the shear velocity = $\sqrt{gS_fh}$ (m/s)
V	reach average velocity (m/s), measured via harmonic tracer travel time and flow path length
V_h	tracer velocity computed as an harmonic average (m/s)
V_{H2O}	volume of water in reach, computed using reach sections (m^3)
V_p	tracer velocity computed using travel times computed as difference between peaks (m/s)
V_w	volume of non-step instream wood (m^3)
V_*	dimensionless velocity = $V/\sqrt{gD_c}$
V^{**}	dimensionless velocity = $V/\sqrt{gSD_c}$
Wd	mean wood "depth" (m) = wood volume/bankfull channel planform area
σ_h	standard deviation of the thalweg depth (m)
σ_y	standard deviation of the residuals of a bank profile regression (m)
σ_z	standard deviation of the residuals of a thalweg longitudinal profile regression (m)

practical tools for predicting flow velocity in natural and constructed channels.

Recently, researchers have been making progress towards developing more accurate methods for predicting velocity in high-gradient channels through the use of dimensionless equations scaled by a value that represents the roughness element size (Rickenmann, 1994; Aberle and Smart, 2003; Ferguson, 2007; Comiti et al., 2007; Comiti et al., 2009; Zimmermann, 2010). With the exception of Zimmermann (2010), these methods rely upon characteristic grain size for roughness scaling. These quantitative methods for predicting velocity and hydraulic resistance have focused on methods that are applicable for step-pool and cascade channels that are primarily formed by clasts, with minimal instream wood present. However, steps in natural channels are often formed through a combination of clasts and wood, which together increase step heights and flow resistance (Kaufmann, 1987; David et al., 2011). For general prediction, methodologies that explain flow resistance through steps formed by both clasts and instream wood, and clasts alone, are needed. Additionally, both resistance coefficients (for energy loss and velocity estimates) and direct velocity prediction are currently required by practitioners, while researchers have primarily shifted their focus to velocity prediction.

In this study, we use a high-resolution dataset collected in Colorado in combination with field datasets collected in the Cascades (Washington State) and the Italian Alps to address two primary objectives: (1) to assess the strengths and weaknesses of existing methods for predicting velocity in high-gradient channels; and (2), to develop generally-applicable methods for velocity prediction in high-gradient channels that have steps composed of clasts, a combination of clasts and wood, and bedrock, through both resistance coefficients and direct velocity estimation.

2. Background

Flow resistance can be separated into three fundamental components: grain, form, and spill. In lower-gradient channels grain resistance is often dominant, though dune-bed channels can be a substantial exception. Form resistance is caused by secondary currents and eddying and has many sources, including bed and bank variability and obstacles such as boulders, bridge piers and instream wood. Spill resistance results from a sudden flow deceleration from supercritical flow, where rapid flow and impinging jets impact on slow-moving water, resulting in hydraulic jumps and substantial turbulence. Form and spill resistance represent local energy losses while grain resistance is a continuous loss due to skin friction and form drag. Grain, form and spill resistance are all interrelated phenomena, though are helpful descriptors of resistance processes. In step-pool and cascade streams (Montgomery and Buffington, 1997), spill resistance is typically dominant (Kaufmann, 1987; Curran and Wohl, 2003; MacFarlane and Wohl, 2003; Wilcox et al., 2006; Kaufmann et al., 2008; Comiti et al., 2009; David et al., 2011). Kaufmann (1987) found that grain resistance accounted for as little as 2–7% of resistance in channels with abundant wood and steps. Wilcox et al. (2006) attributed 68% and 92% of the total resistance to spill, while grain resistance was found to contribute only 8–32% of the total. David et al. (2011) found that spill resistance generally contributed the most towards total resistance in high gradient step-pool and cascading streams, and that the contribution of spill was reduced at high flows.

The Manning and Darcy-Weisbach equations are the most common approaches for velocity prediction in open channels, through the use of the flow resistance coefficients n and f. These coefficients typically represent average reach conditions; they are composite

values that include all resistance components. The Manning and Darcy-Weisbach equations are:

$$V = \frac{R^{2/3} S_f^{1/2}}{n} = \sqrt{\frac{8gRS_f}{f}} \tag{1}$$

where V is the average reach velocity (m/s); n is the Manning's coefficient; f is the friction factor; S_f is the friction slope (m/m); g is the acceleration due to gravity; R, the hydraulic radius, is computed as A/P_w; A is the cross-sectional area (m^2); and P_w is the wetted perimeter (m). To estimate reach-average velocity, all other terms must also be reach-averaged values. The Darcy-Weisbach equation was originally developed for pressurized conduits, though it has been argued to be the more appropriate roughness coefficient for general use in open-channel hydraulics. The friction factor has the advantage of being dimensionless while the Manning coefficient has the unsatisfying dimensions of $time * length^{-1/3}$. The Manning's equation has been argued to be a poor choice for velocity prediction (Ferguson, 2010). Both f and n are used in computational modeling but n remains the most applied method.

There are various quantitative methods developed in the field and laboratory that are potentially applicable for estimating velocity and resistance coefficients in high-gradient channels (Table 1). Methods predicting flow resistance coefficients based on field data from natural channels exist for both Manning's n (Jarrett, 1984; Rickenmann, 1994) and Darcy-Weisbach f (Bathurst, 1985; Kaufmann, 1987; Mussetter, 1988; Comiti et al., 2007; Kaufmann et al., 2008). Additionally, techniques for the direct estimation of velocity have been developed using both field data (Jarrett, 1984; Rickenmann, 1994; Ferguson, 2007; Comiti et al., 2007) and laboratory data on self formed steps (Comiti et al., 2009; Zimmermann, 2010). From laboratory data, flow resistance has been investigated in high-gradient channels on self-formed steps (Aberle and Smart, 2003), including a study that combined field data with a flume study (Lee and Ferguson, 2002). For the design of engineered channels, the flow resistance of rip rap bed material on high-gradient slopes has also been investigated (Thompson and Campbell, 1979; Abt et al., 1988; Rice et al., 1998), including rock chutes with protruding boulders (Pagliara and Chiavaccini, 2006) that can be used as grade stabilization structures. However, there can be a fun-

damentally different morphology between natural and such engineered channels, with a result of differing physical processes (e.g., dominance of form over spill resistance) leading to energy dissipation. Data gathered in engineered channels may belong to different populations than natural step-pool channels and prediction methodologies may not be transferable between these populations.

There is no single approach in these highly-variable channel types that can confidently be applied for prediction, partly due to reliance upon characteristic grain size in systems that include such complications as the influence of instream wood. Natural channels with instream wood have taller steps, finer sediments, higher flow resistance and lower velocities (Comiti et al., 2008; David et al., 2010b, 2011). In high-gradient streams researchers have found that relative submergence using D_{84} is a poor predictor of overall resistance (Curran and Wohl, 2003; MacFarlane and Wohl, 2003; Comiti et al., 2007; David et al., 2010a), though step D_{84} has been shown to be moderately effective (Lee and Ferguson, 2002). A bed-form submergence term that quantified bedform irregularity, specifically the standard deviation of thalweg depths (σ_z) and thalweg residual depth (d_{res}), was tested by Kaufmann (1987) with moderate success. More recently, a detrended bed irregularity index, the standard deviation of the residuals of a bed profile regression (σ_z), has been highly correlated with flow resistance from longitudinal profiles in self-formed experimental channels (Aberle and Smart, 2003), though Reid and Hickin (2008) found poor correlation between a measure of form resistance and σ_z and Comiti et al. (2007) did not find σ_z to be advantageous over D_{84} for prediction. Additionally, the standard deviation of three-dimensional bed elevations in a sand-bedded river has been well correlated with discharge and may be a more effective measure of bed roughness than bedform height (Aberle et al., 2010). Previously, flow resistance has been predicted using the predictor residual depth (Kaufmann, 1987), with the contribution of instream wood also included (Kaufmann et al., 2008).

Researchers have implemented a non-dimensional approach with unit discharge to estimate velocity (Rickenmann, 1994; Ferguson, 2007; Comiti et al., 2007; Comiti et al., 2009; David et al., 2010a; Zimmermann, 2010). Specifically, dimensionless velocity (V^*) has been found to be well correlated with dimensionless unit discharge (q^*), where

Table 1
Data characteristics and equations of high-gradient velocity and low resistance prediction methodologies, based upon laboratory- and field-collected data. The Vel. column indicates the velocity measurement technique used in each analysis, where (a) refers to the use of stream-gaging techniques and section area for velocity computations; and (b) refers to the use of a tracer to measure average reach velocity. '–': not relevant or insufficient data available. For the variable definitions, refer to the notation section.

Method	Data points	Slope (%)		n		f		V (m/s)		Vel. Mthd.
		Min.	Max.	Min.	Max.	Min.	Max.	Min.	Max.	
Thompson and Campbell (1979) $f = \sqrt{\frac{(1-0.1k_s)}{R}\left(2\log\left(\frac{12R}{k_s}\right)\right)}$ $k_s = 4.5D_{50}$	26	0.37	5.2	–	–	0.085	0.94	–	–	(a)
Jarrett (1984) $n = 0.32 S_f^{0.38} R^{-0.16}$ $V = 3.1 R^{0.83} S_f^{0.12}$	75	0.2	3.4	0.028	0.16	0.16	6.7	0.27	2.6	(a)
Bathurst (1985) $\sqrt{\frac{8}{f}} = 5.62\log\left(\frac{\bar{h}}{D_{84}}\right) + 4$	44	0.4	3.7	0.027	0.19	0.06	5.5	0.17	3.6	(a)
Kaufmann (1987) A : $\sqrt{\frac{8}{f}} = 0.62\ln\left(\frac{d_{th}}{d_{res}}\right)$ B : $\sqrt{\frac{8}{f}} = \ln\left(\frac{d_{th}}{\sigma_h}\right)^{0.92}$	40	2.6	8.3	0.1	0.76	2.0	87	–	–	(b)
Rickenmann (1994) $V = 0.37\frac{g^{0.33} Q^{0.34} S_o^{0.2}}{D_{90}^{0.35}}$ $\frac{1}{n} = 0.56\frac{g^{0.44} Q^{0.11}}{S_o^{0.33} D_{90}^{0.45}}$	217	0.8	63	–	–	–	–	–	–	(a,b)
Rice et al. (1998) $n = 0.080(D_{50}S_o)^{0.15}$	21	2.5	33	~0.023	0.048	0.16	0.82	–	–	(a)
Lee and Ferguson (2002) $\sqrt{\frac{1}{f}} = 1.48\left(\frac{R}{D_{84}}\right)^{1.80}$ D_{84}: step grain size	81	2.6	18	0.06	8.0	0.5	~5000	0.02	0.67	(b)
Aberle and Smart (2003) $\sqrt{\frac{8}{f}} = 0.91\frac{\bar{h}}{\sigma_z}$	94	2.0	10	–	–	~0.07	~6	~0.1	~1.1	(b)
Comiti et al. (2007) $f = 87.1 q^{*-0.50} S_f^{1.83}$ $q^* = \frac{q}{\sqrt{gD_c^3}}$ $D_c = D_{84}$ $V^* = 0.92q^{*0.66}$	44	8.0	21	–	–	1.8	28	0.22	1.4	(b)
Ferguson (2007) $V^* = 1.44q^{*0.6} S_o^{0.2}$ $V^* = \frac{V}{\sqrt{gD_c}}$	376	0.07	21	–	–	–	–	~0.03	~3	(a,b)
Kaufmann et al. (2008) $\frac{f}{8} = 1.21 d_{res}^{1.08}(d_{res} + Wd)^{0.638} d_{th}^{-3.32}$	36	2.6	8.3	0.10	0.76	2.0	87	–	–	(b)
Comiti et al. (2009) $V^* = 1.24q^{*0.83}$	205	8.4	14	–	–	–	–	~0.1	~1.2	(b)
Zimmermann (2010) $V^* = 0.58q^{*0.39}$	139	0.03	0.23	–	–	–	–	0.17	1.07	(b)

$$V^* = \frac{V}{\sqrt{gD_c}} \tag{2}$$

$$q^* = \frac{q}{\sqrt{gD_c^3}} \tag{3}$$

and D_c is a roughness parameter. Rickenmann and Recking (2011) modified dimensionless velocity and unit discharge by adding slope to the denominator, specifically:

$$V^{**} = \frac{V}{\sqrt{gS_fD_c}} \tag{4}$$

$$q^{**} = \frac{q}{\sqrt{gS_fD_c^3}} \tag{5}$$

Additionally, dimensionless discharge (Q^*),

$$q^* = \frac{Q}{D_c\sqrt{gD_c^3}} \tag{6}$$

may also have application for prediction (Parker et al., 2007). With an assumption that D_c is equivalent to D_{84}, velocity has been predicted with relatively high levels of explained variance in self-formed laboratory channels that lack instream wood. However, since D_{84} has been shown to be a poor predictor of overall resistance in these stream types (David et al., 2010a), the use of a different roughness parameter may be more appropriate in streams with substantial bedforms (Aberle and Smart, 2003; Zimmermann, 2010), especially in channels that have instream wood increasing step heights. Furthermore, methods that provide predictions in channels both with and without instream wood are most helpful for general application. A bed irregularity index, such as σ_z, is appropriate in this application, since it captures the influence of all sources of bed variability and not just variability due to the largest clast sizes.

With its potential descriptive power, the standard deviation of bed elevations (σ_z) may be a useful tool for addressing this challenge of general prediction, as the roughness term in relative submergence and dimensionless discharge. Using a field-collected database of velocity and geometric characteristics, we assessed the strengths and weaknesses of existing prediction methods and used these strengths in the development of new methodologies for velocity prediction in high-gradient channels.

3. Methods

We collected average reach velocity data in 15 natural high-gradient channels using a Rhodamine WT tracer. These data were used in combination with detailed surveys of channel geometry and water surface profiles to compute n and f. A summary of the field data collection methodologies is provided below. For additional details on these techniques, see Yochum (2010) and David et al. (2010a). Additionally, data collected by Curran and Wohl (2003), MacFarlane and Wohl (2003), and Comiti et al. (2007) were used in the analysis; we also present summaries of their methodologies.

3.1. Field study area

Data collection was performed in the US Forest Service (USFS) Fraser Experimental Forest, in three watersheds of East Saint Louis (ESL) Creek and Fool Creek (FC). Watershed areas ranged from 0.69 to 8.5 km², with streamflow dominated by snowmelt. The Fraser Experimental Forest is located in the Upper Colorado Basin west of the town of Fraser, approximately 115 km west of Denver, Colorado,

USA (Fig. 1). Discharge was measured by the USFS using sharp-crested weirs. Data were collected on five cascade, eight step-pool, one transitional, and one plane-bed stream reaches, with slopes ranging from 1.5% to 20%. Instream wood was present in all reaches, both within the steps and dispersed throughout the reaches. With lengths ranging from 6 to 35 m, some of the reaches were relatively short but were initiated and terminated at similar bedform points and had consistent morphology, depth variability, and wood loading throughout. The clasts anchored the instream wood, increasing step
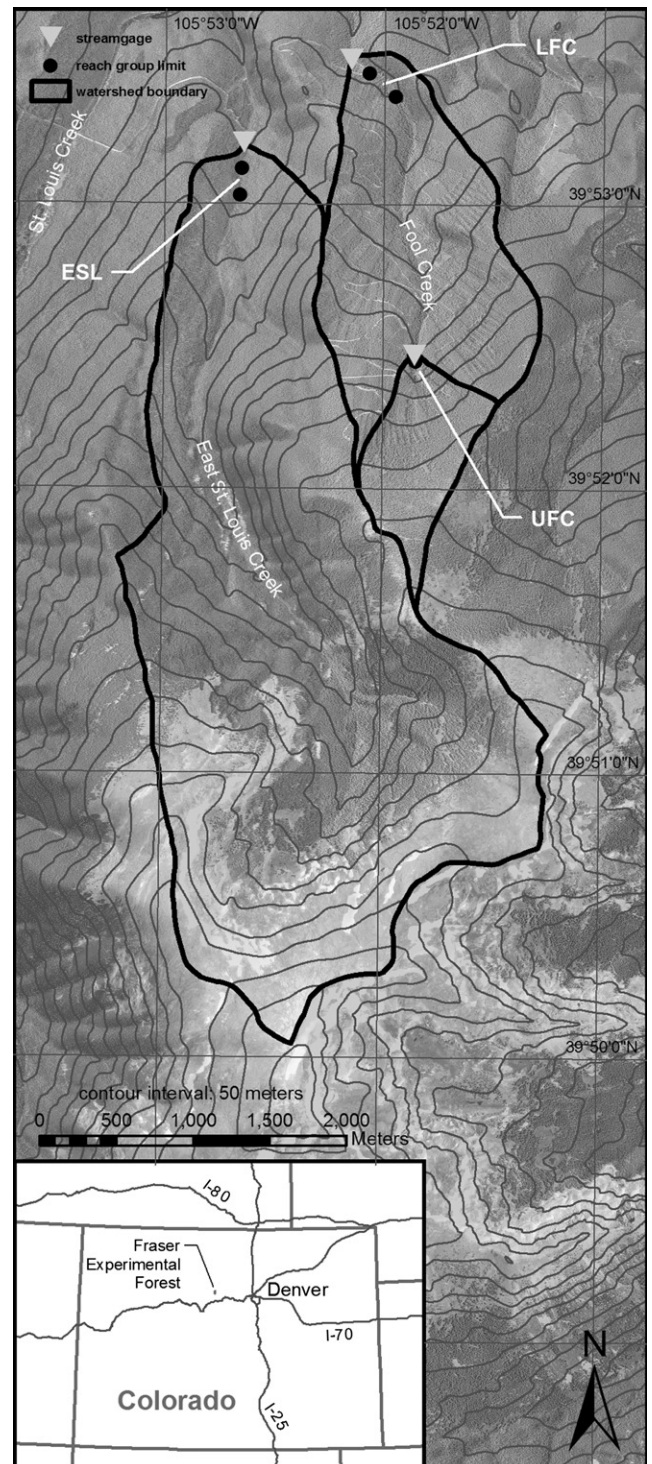

Fig. 1. Research watersheds and stream reaches, Fraser Experimental Forest, Colorado, USA. ESL: East Saint Louis Creek; LFC: Lower Fool Creek; UFC: Upper Fool Creek.

Fig. 2. Photographs of East Saint Louis (ESL) Creek, reach 1 (left) and reach 4 (right).

heights, bed variability and flow resistance. Typical channel characteristics are illustrated in Fig. 2; additional photographs are available (Yochum, 2010; Yochum and Bledsoe, 2010).

Data collection was composed of longitudinal water surface profiles, at high, medium, and low flows; bed, bank, and floodplain topographic surveying; bed-material characterization using a pebble count; and average reach velocity measurements. Measurements were collected during flows ranging from 23% to 570% of the average mean daily discharge. Near-bankfull measurements were made at flows equivalent to the 1.1- to 2.1-yr return period, as defined by log-Pearson Type III frequency analyses of streamgage records.

3.2. Channel geometry surveys

Reach surveying was performed with a terrestrial LiDAR scanner for above-water surface features and a gridded total station survey for below-water features. Channel reach lengths varied from 6.2 to 35 m, with flow widths from 0.7 to 4.0 m. The Leica HDS Scanstation system was used for collecting the LiDAR data. Each of the fifteen reaches was scanned from multiple directions to minimize shadow. A key advantage of LiDAR is that this surveying technique allows a virtual revisit and resurvey of channel characteristics at any time. From the LiDAR scans and additional total station data, cross sections were developed at an interval of 0.75 to 1.50 m over the 6- to 35-m reach lengths, for a total of nine to 27 sections for each reach. Longitudinal profiles of the bed and water surface were measured using a total station during each resistance measurement. The longitudinal profiles were collected at the thalweg, and left and right edges of water, with uniform spacing at an interval of 0.29 m for the thalweg. Bed gradation was measured using a 300-point, spatially-referenced pebble count. The slope of the water surface was assumed to be equivalent to S_f and was computed using the upstream and downstream water surface elevations and the length of the longitudinal profile, with reaches starting and ending in comparable positions.

The detrended standard deviation of bed elevations (σ_z) was computed from total station surveyed 2-dimensional longitudinal profiles by performing a linear regression of bed elevations versus distance and computing the standard deviation of the regression residuals. The average edge of water sinuosity (K_b) was computed as the average of the left and right bank sinuosity, which were measured using edge of water longitudinal profiles and computed as the measured edge-of-water length divided by a straight line distance in these relatively short reaches. Analogous to σ_z, the standard deviation of the residuals of a bank profile regression (σ_y) was computed using the edge-of-water longitudinal profiles by defining a thalweg-aligned vertical reference plane and performing a linear regression of y-distance (perpendicular to stream axis, in a horizontal plane) versus the longitudinal distance. Finally, non-step instream wood density was computed as the volume of the submerged non-step instream wood (V_w, as measured from the LiDAR data), divided by the flow volume of the reach (V_{H2O}). Low flow data were excluded from computations involving instream wood, to avoid inaccuracies induced from extrapolations from the LiDAR below the low flow water level.

Ratios of depth to σ_z, a relative submergence variable, were used to predict velocity and resistance coefficients. Since this ratio can describe bed elevation variability in all stream types that express bedform, including microforms (Hassan and Reid, 1990) in gravel bed channels as well as variability in sand bed channels (Aberle et al., 2010), h/σ_z is a general descriptor and can be termed relative bedform submergence (in contrast to relative grain submergence, R/D_{84}). Since σ_z is dependent upon the resolution of the longitudinal profile, a sensitivity analysis of the profile spacing was performed to assess the influence of spacing variability upon the predictions, with 3/4, 1/2, and 1/4 of the longitudinal points used to predict f. Spacing was described using a dimensionless channel width/spacing ratio, where average wetted flow width is divided by the average spacing of the thalweg longitudinal profile.

3.3. Velocity measurements

Average reach velocities were computed as the thalweg flow path length divided by the travel time. The travel time was measured using Rhodamine WT dye, with replicates of four to five

injections per resistance measurement to address potential error associated with signal noise. The Rhodamine WT was measured at a 1-s time step using two synchronized fluorometers mounted to rebar in the thalweg at the reach limits. The dye was released as a slug in midstream. Travel time was computed using a spatial harmonic mean travel time, which has been argued as being the most appropriate method under steady flow conditions (Walden, 2004; Zimmermann, 2010). Details of the methodology are provided in Yochum (2010). To address data noise due to sunlight and aeration, a single-pass 3-point median smoothing methodology was applied to the Rhodamine WT data. Median smoothing, suggested by Tukey (1974), tends to preserve sharp signal edges while filtering out impulses (Gallagher and Wise, 1981; Ataman et al., 1981). Froude numbers were calculated using the average velocity, flow area and top width for each reach.

These velocities are updated values compared to those presented by David et al. (2010a,b, 2011), with resulting shifts in flow resistance coefficients. Specifically, this work employs a dataset resulting from the use of harmonic as opposed to centroid travel times, the use of smoothed tracer data to reduce the influence of excessive noise from aeration and sunlight interactions with the fluorometers, and the elimination of outlying replicate travel times.

3.4. Analysis of additional datasets

Data collected by several other researchers in high-gradient channels were used to extend the Fraser dataset, as described above. This aggregated dataset includes alluvial channels without instream wood (MacFarlane and Wohl, 2003; Comiti et al., 2007), alluvial channels with instream wood (Yochum, 2010; Curran and Wohl, 2003), mixed alluvial and bedrock channels (Yochum, 2010; MacFarlane and Wohl, 2003; Curran and Wohl, 2003), and bedrock channels (MacFarlane and Wohl, 2003). Hence, these data were collected in channels with and without instream wood present to potentially enhance step heights.

The Curran and Wohl (2003) dataset consists of 20 low flow measurements in step-pool streams with instream wood in the Cascade Range, Washington, USA. The reaches spanned slopes between 7% and 18%, lengths from 46 to 74 m, and beds composed of alluvium or a combination of alluvium and bedrock. Discharge was not measured. Longitudinal profiles and 10 cross-sections were measured for each reach, with the sections placed fairly uniformly, in both steps and pools. Flow velocity data were collected using a salt tracer and conductivity probes, with travel times computed using a difference in tracer peak concentrations.

The MacFarlane and Wohl (2003) dataset consists of 20 low flow measurements in 15 step-pool streams on the Western Slope of the Cascade Range, Washington. The reaches spanned slopes between 4% and 18%, lengths from 39 to 69 m, and with beds composed of alluvium, a combination of alluvium and bedrock, or bedrock. Little to no instream wood was present and discharge was also not measured. Longitudinal profiles and 10 equally-spaced sections were measured for each velocity measurement, with the sections in both steps and pools. Flow velocity data were collected using a salt tracer and conductivity probes, with travel times computed using a difference in tracer peak concentrations.

The Comiti et al. (2007) dataset was collected in the Rio Cordon, in the Eastern Italian Alps. The reaches consisted of cascade and step pool channels with slopes ranging from 7.9% to 21%. Reach lengths varied from 16 to 76 m. Discharge during data collection ranging from 0.077 to 1.86 m³/s, with a maximum flow at approximately 80% of the bankfull discharge. In contrast to the Fraser and Curran and Wohl (2003) reaches, the Rio Cordon reaches have less-developed bedforms, likely due to the long term practice of instream wood removal and low recruitment due to high-elevations.

Longitudinal profiles and three sections per reach were measured to characterize the channel geometry. These few sections were not placed at a uniform interval throughout each reach but were instead placed at intermediate locations between pools and steps, avoiding boulders and other irregularities. The resulting section characteristics likely represent a different population than those characteristics provided by regular-interval reach sections, which will impact flow resistance values. Flow velocity data were collected using a salt tracer, with conductivity probes logging at an acquisition step of 5 s and travel times computed using a difference in tracer peak concentrations.

There is a systematic bias induced to the velocity and resistance coefficient calculations by the use of difference in concentration peaks for the travel time computations, as opposed to a harmonic average. Using the Fraser tracer data, both harmonic and peak flow velocities were computed and the results were compared. On average, velocities computed using the difference in tracer peak concentrations (V_p) overpredicted the harmonic velocities (V_h) by 12.4%. Using this finding as a conversion allows translation ($V_h = 0.876V_p$) of the additional datasets into a consistent form.

3.5. Statistical analyses

Existing methods for predicting flow resistance coefficients were tested on the Fraser database to assess their relevance in these stream reaches. Additionally, simple linear and multivariate regressions were performed on the assembled dataset, to search for effective explanatory variables for predicting flow resistance and for illuminating flow resistance processes. Statistical analyses were performed using the software R (version 2.10.1). Tested explanatory variables described bed material, slope, and bed and bank variability. Natural logarithmic transformations were applied, which provided good adherence to the regression assumptions of linearity, homoscedasticity, and independent and normally-distributed residuals.

Equations for predicting velocity, Manning's n and Darcy-Weisbach f were tested (Table 1). Performance of the regression models was assessed through the coefficient of determination (R^2), while predictive performance was assessed through the root mean square (RMS) error of the Fraser data, in normal, not log transformed space. RMS error is computed as:

$$RMS = \sqrt{\frac{\sum(predicted - measured)^2}{N}} \tag{7}$$

For models that have the most potential for use in prediction, 95% prediction intervals were computed to quantify the expected variability in estimates.

4. Results

Relatively low velocities were measured in the 15 high-gradient Fraser stream reaches (Table 2), with subcritical reach-average Froude numbers in channels with slopes from 1.5% to 20% and flow resistance coefficients substantially higher than standard tabular values from many traditional engineering references (Chow, 1959; Brunner, 2010). Measured average reach characteristics are provided in Table A1. The average Manning's n was 0.18 for near-bankfull flow. Flow resistance varied substantially by stage, with lower resistance coefficients computed for higher flow rates. A summary of the measurements collected by Curran and Wohl (2003), MacFarlane and Wohl (2003), and Comiti et al. (2007), with velocity and resistance coefficient adjustments for the harmonic average, is provided (Table 3).

Table 2
Range of measured average reach velocities, flow resistance coefficients and Froude numbers for the Fraser stream reaches.

	Velocity (m/s)	Manning's n	Darcy-Weisbach f	Froude #
Near-bankfull flow	0.51–1.32	0.05–0.30	0.28–11	0.30–0.77
Mid-flow	0.18–0.61	0.08–0.40	0.67–26	0.15–0.38
Low flow	0.11–0.40	0.10–0.52	1.4–56	0.13–0.31

Table 3
Range of corrected (for the harmonic average) reach velocities and flow resistance coefficients for the additional datasets.

	Slope (m/m)	Velocity (m/s)	Mannings n	Darcy-Weisbach f
Curran and Wohl (2003)	0.06–0.18	0.038–0.46	0.21–1.7	6.3–480
MacFarlane and Wohl (2003)	0.05–0.14	0.046–0.25	0.27–0.76	14–130
Comiti et al. (2007)	0.08–0.21	0.20–1.2	0.13–0.50	2.2–38

4.1. Resistance coefficients prediction

For each of the previously published relationships tested (Table 1), plots of measured versus predicted values and RMS error for both overall and slope-binned fits are provided (Fig. 3). In general, existing flow resistance prediction equations substantially underpredict flow resistance of the Fraser channels. For n prediction, the models developed by Jarrett (1984) and Rickenmann (1994) performed best (Fig. 3a and d). Predictions using Jarrett (1984) have lower RMS error than Rickenmann (1994), but have more bias about the line of perfect agreement at higher resistances. The Aberle and Smart (2003) model provided the most accurate predictions of f (Fig. 3i), though the model developed by Kaufmann et al. (2008) performed well. Comiti et al. (2007) consistently followed the trend of the data, though had a systematic bias in the predictions. The bedform submergence equation developed by Kaufmann (1987), implementing d_{th}/σ_d, performed moderately well (Fig. 3f). The least accurate predictions were made by the Rice et al. (1998) model for n, and Bathurst (1985) and Lee and Ferguson (2002) models for f, with substantial biases indicated in the measured versus predicted plots for the full range of predictions. The Thompson and Campbell (1979) model also provided a poor fit for f (Fig. 3b), with the Fraser dataset clearly belonging to a different population than the data used to derive this predictive equation.

Using the Fraser database, relative bedform submergence, in the form of R/σ_z, predicted up to 80% of the variability in f (Table 4, model 2). Relative bedform submergence in the form of h_m/σ_z, which can be more-easily measured a priori, explained the same level of variability (models 3 and 4), while both methods performed substantially better than prediction methods based upon relative grain submergence ($R^2 = 0.40$). With σ_z computed from longitudinal profile regressions, the method detrends the profiles to exclude the influence of slope. Edge of water sinuosity (K_b) explained far less variability in the data ($R^2 \leqslant 0.43$, models 5 and 6), as was the case with R/σ_y (models 7 and 8). Non-step instream wood density, which ranged from nearly 0–4.3%, explained little variance in the dataset ($R^2 < 0.05$).

Using variables describing bedforms, bankforms, and non-step instream wood, multivariate regression models were tested to assess the variance of the Fraser dataset that can be explained with a suite of descriptors. Adding bank sinuosity to relative bedform submergence increased the explained variance for n and f to 0.83 and 0.84, respectively (Table 4, models 9 and 10). R/σ_y was not significant when added to relative bedform submergence ($\alpha = 0.05$). Non-step instream wood density was also not significant in the multivariate regressions, despite indicating low correlation with relative bedform submergence ($r = -0.17$). Relative bedform submergence and bank sinuosity are weakly correlated ($r = -0.47$) while R/σ_y indicates more substantial correlation ($r = 0.71$) with relative bedform submergence. Bedform and bankform, as expressed by these variables, have a limited level of interdependence in the Fraser dataset.

Adding low flow data collected in the Cascades had a variable effect on the regressions. With the addition of the MacFarlane and Wohl (2003) dataset, the explained variance initially dropped ($R^2 = 0.73$ for n vs. R/σ_z), but with the elimination of a bedrock-bed, shallow flow outlier (as identified in Q–Q plots), the explained variance increased to 0.80 for n and 0.84 for f (models 11 and 12). Similar results were found for regressions with h_m/σ_z (models 13 and 14, Fig. 4). The addition of the Curran and Wohl (2003) dataset, which includes channels with substantial instream wood, both within steps and dispersed throughout the channels (Curran 1999), decreased the model R^2 values using R/σ_z for n and f to 0.69 and 0.73, respectively, with less substantial reductions found using h_m/σ_z.

The density of longitudinal survey points affected the accuracy of f prediction (Table 5). Using 3/4, 1/2, and 1/4 of the longitudinal points in the Fraser database varied the point density from an average of 0.28 to 1.05 m, with the average channel width/spacing ratio ranging from 7.9 to 2.2. Reducing the point density by 25% and 50% reduced the R^2 from 0.80 to 0.78 and 0.79, respectively. With a reduction to an R^2 of 0.74, point density reductions of 75% (1/4 points) had a more substantial negative influence upon the predictions, though this result could be biased by the impact of reduced sample sizes in channels of variable lengths on standard deviation computations.

4.2. Direct velocity prediction

Previously published methods for the direct prediction of velocity were assessed using the Fraser dataset. In general, the previously published models overpredict velocity measured in the Fraser (Fig. 5), analogous to resistance coefficients being underpredicted. An equation developed by Zimmermann (2010) with flume data, which used $D_c = \sigma_z$, provided predictions with the lowest RMS error (Fig. 5f), though a small systematic bias is indicated. Additionally, the methods presented by Rickenmann (1994) and Jarrett (1984) provided relatively low RMS error (Fig. 5a and b), though both show considerably more scatter than Zimmermann (2010) and also show a consistent underprediction bias. The methods developed by Ferguson (2007), Comiti et al. (2007) and Comiti et al. (2009) all predicted velocity with high RMS error and showed inconsistent bias, with greater underprediction error for higher velocities.
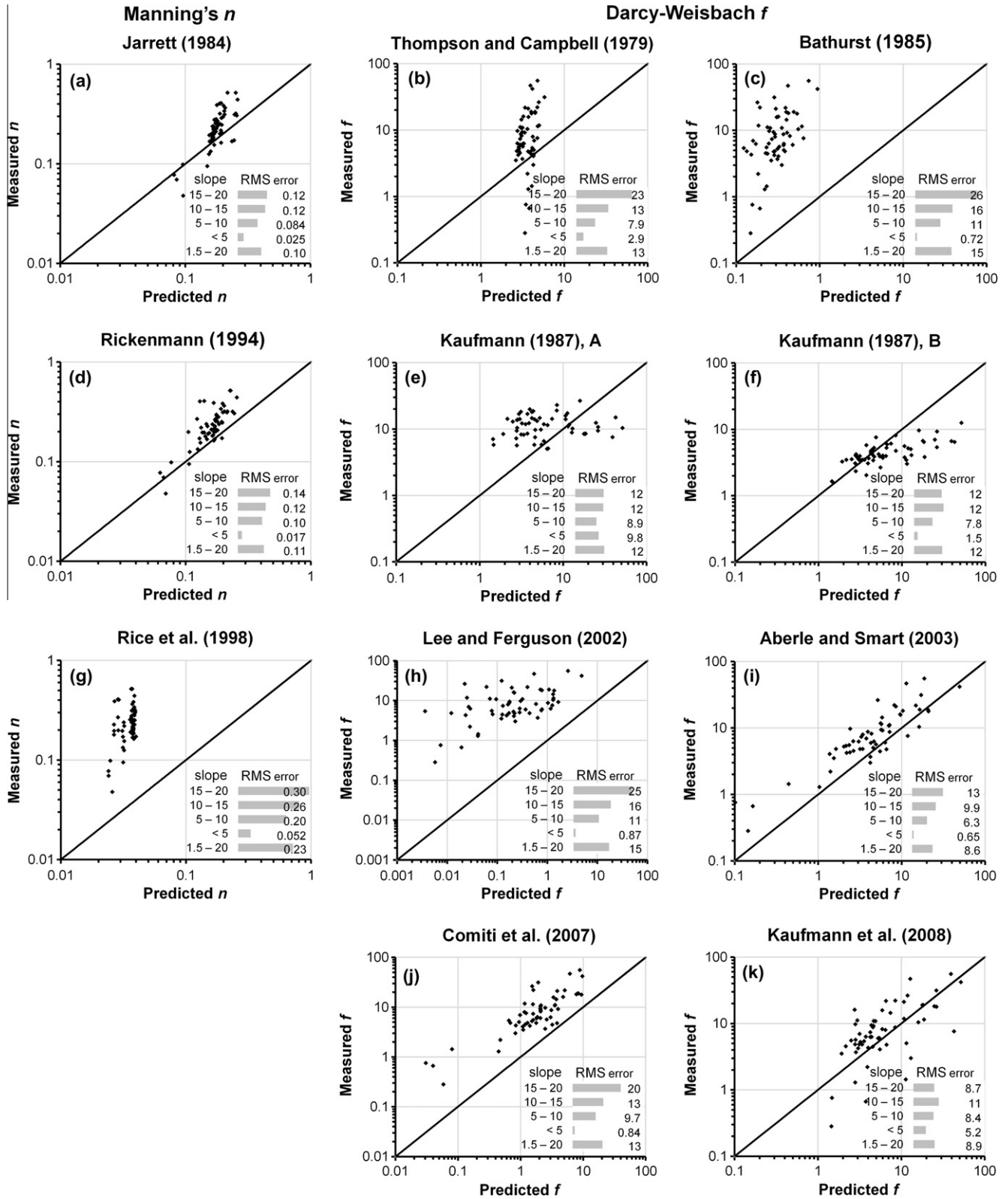
Fig. 3. Evaluation of existing methods for predicting flow resistance coefficients, with plots of measured versus predicted values and RMS error for overall and slope-bracketed fits. The solid line indicates the position of perfect agreement between measured and predicted values.

Additionally, optimized methods were developed using the Fraser and other field-collected datasets. Using the finding that σ_z is more generally applicable than D_{84}, methods implementing V^* and V^{**}, with $D_c = \sigma_z$, were tested for their predictive capabilities

for estimating velocity with a known discharge (Table 6). Using the Fraser database, V^* was estimated using q^* (Table 6, model 15), with 93% of the variance explained and an overall RMS error for predicted versus measured velocity of 0.071 m/s. The use of

Table 4
Flow resistance coefficient prediction equations, using relative bedform submergence and bank sinuosity. N refers to the number of data points used in the model while # refers to the model number.

Explanatory Variables: a, b	N	Manning's n				Darcy-Weisbach f			
		#	R^2	Adj-R^2	Equation	#	R^2	Adj-R^2	Equation
R/σ_z	59	1	0.76	–	$n = 0.25(a)^{-0.67}$	2	0.80	–	$f = 9.7(a)^{-1.49}$
h_m/σ_z	59	3	0.76	–	$n = 0.43(a)^{-0.76}$	4	0.80	–	$f = 32(a)^{-1.79}$
K_b	59	5	0.43	–	$n = 0.10(a)^{3.10}$	6	0.34	–	$f = 1.7(a)^{5.91}$
R/σ_y	59	7	0.35	–	$n = 0.13(a)^{-0.37}$	8	0.40	–	$f = 2.3(a)^{-0.85}$
$R/\sigma_z, K_b$	59	9	0.83	0.83	$n = 0.17(a)^{-0.56}(b)^{1.50}$	10	0.84	0.83	$f = 5.5(a)^{-1.32}(b)^{2.18}$
R/σ_z	78	11	0.80	–	$n = 0.25(a)^{-0.67}$	12	0.84	–	$f = 9.9(a)^{-1.51}$
h_m/σ_z	78	13	0.78	–	$n = 0.41(a)^{-0.69}$	14	0.82	–	$f = 29(a)^{-1.56}$
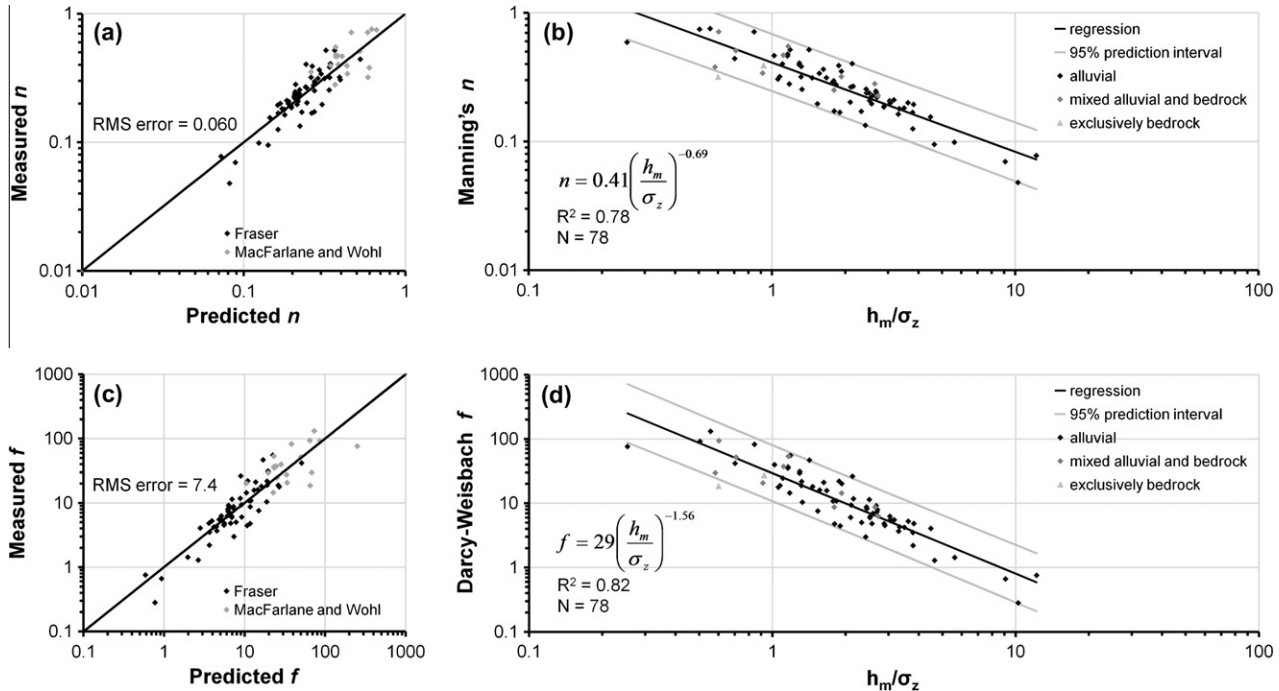
Fig. 4. Measured versus predicted performance and regressions for predicting resistance coefficients using relative bedform submergence, based on the Fraser, and MacFarlane and Wohl (2003) datasets. Ninety-five percent prediction intervals are provided, with RMS error computed in normal space using only the Fraser database.

Table 5
Longitudinal spacing sensitivity analysis for the Darcy-Weisbach f, for the Fraser dataset.

Longitudinal points	Average spacing (m)	Average width/spacing	R^2	F-value
All	0.28	7.9	0.80	222
¾	0.38	6.0	0.78	205
1/2	0.55	4.1	0.79	209
1/4	1.05	2.2	0.74	162

Q^* (Parker et al., 2007) in place of q^* (model 16) reduced the explained variance ($R^2 = 0.88$) and increased the RMS error (0.096 m/s). The use of an additional modified dimensionless form, which incorporates a slope term in addition to D_c (Rickenmann and Recking, 2011), explained the most variance ($R^2 = 0.97$), though the RMS error was slightly higher, at 0.072 m/s (model 17). The dataset of Comiti et al. (2007) was added to the analysis to assess how high-gradient stream reaches without instream wood affect prediction accuracy. With the addition of these data, the predictive equations did not substantially change, with similar coefficients and RMS error for the Fraser database (models 18 through 20). The highest explained variance was 93% (Fig. 7a and b), with an associated RMS error of 0.076.

Relative bedform submergence was also tested for the direct prediction of velocity for situations in which discharge is unknown. Using the Fraser database of channels with instream wood, V^* and V^{**} were predicted with 81% and 90% of variance explained, respectively (Table 5, models 21 and 22). With the addition of the non-instream wood dataset (MacFarlane and Wohl, 2003), explained variance increased slightly (models 23 and 24), with up to 91% of the variance explained (Fig. 6c and d), though RMS error increased slightly to 0.12 m/s. The use of the R/σ_z version of relative bedform submergence (model 25) increased explained variance (94%) and decreased RMS error (0.10 m/s). Expanding the database further to include the Curran and Wohl (2003) dataset of channels with both step-forming and non-step instream wood reduced the explained variance for h_m/σ_z to 88%.

5. Discussion

This study indicates that both relative bedform submergence and dimensionless unit discharge (with $D_c = \sigma_z$) are robust predictors of velocity and flow resistance that overcome limitations imposed through use of grain size as the characteristic roughness height in high-gradient channels. Characteristic grain size cannot quantify the influence of instream wood in enhancing step heights,
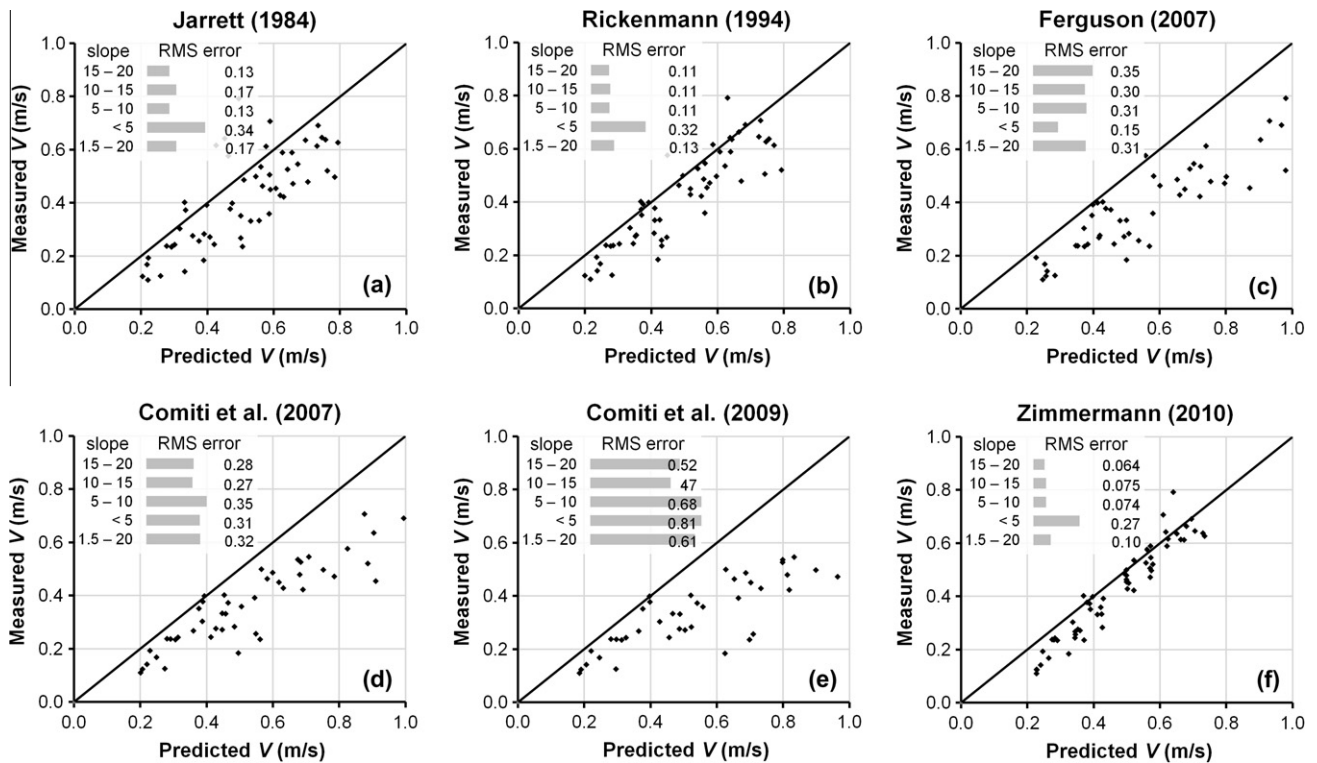
Fig. 5. Evaluation of existing methods for predicting velocity in high-gradient channels, with plots of measured versus predicted values and RMS error. The solid line indicates the position of perfect agreement between measured and predicted values.

Table 6
Velocity prediction equations, using dimensionless velocity and discharge, as well as relative bedform submergence. N refers to the number of data points used in the model while RMS error is computed for only the Fraser database velocities, in normal space. $V^{**} = V/\sqrt{gS\sigma_z}$; $q^* = q/\sqrt{g\sigma_z^3}$; $q^* = q/\sqrt{gS\sigma_z^3}$; $Q^* = Q/(\sigma_z\sqrt{g\sigma_z^3})$.

Model #	N	R^2	RMS	Equation
15	59	0.93	0.071	$V^* = 0.57q^{*0.53}$
16	59	0.88	0.096	$V^* = 0.18Q^{*0.34}$
17	59	0.97	0.072	$V^{**} = 0.97q^{**0.60}$
18	103	0.90	0.071	$V^* = 0.59q^{*0.53}$
19	103	0.87	0.097	$V^* = 0.18Q^{*0.35}$
20	103	0.93	0.076	$V^{**} = 1.0q^{**0.60}$
21	59	0.81	0.116	$V^* = 0.15(h_m/\sigma_z)^{0.98}$
22	59	0.90	0.111	$V^{**} = 0.34(h_m/\sigma_z)^{1.39}$
23	78	0.86	0.124	$V^* = 0.13(h_m/\sigma_z)^{1.10}$
24	78	0.91	0.119	$V^{**} = 0.37(h_m/\sigma_z)^{1.30}$
25	78	0.94	0.101	$V^{**} = 0.90(R/\sigma_z)^{1.25}$

increasing resistance, and decreasing average reach velocity. Grain size is not relevant for describing geomorphic variability in bedrock channels and is insufficient for describing variability in channels with large bedforms. In high-gradient channels, methods based upon σ_z have potential for predicting both resistance coefficients and velocity given a longitudinal profile of sufficient point density to quantify bedform variability.

When there is a need to predict flow velocity and resistance coefficients in high-gradient channels with steps enhanced by instream wood, substantial inaccuracies result when using most previously published methods. For general prediction, methodologies that explain flow resistance through steps formed by both clasts and instream wood, and clasts alone, are needed. Of the previously available methods, the equation developed by Aberle and Smart (2003) provided the best fit to the measured Darcy-Weisbach f values (Fig. 3i). The relevant application of this relationship to the wood-enhanced steps of the Fraser channels is surprising

considering that the Aberle and Smart dataset was developed entirely in the laboratory, on self-formed alluvial steps (Rosport, 1997; Koll, 2002). This suggests that the ratio of depth to σ_z, as relative bedform submergence, provides a transferable scaling relation for flow resistance prediction in high-gradient channels. Similarly, the strong performance of a Zimmermann (2010) model, even though this relationship was developed in the laboratory using only clasts, indicates that these relationships are more generally valid if $D_c = \sigma_z$. With the aid of accounting directly for wood volume, the use of the residual depth method (Kaufmann et al., 2008) also proved to be relatively effective for prediction. However, this method performed less effectively than relative bedform submergence, in general, and substantially overpredicted resistance in channels with the smallest bedforms and underpredicted resistance in channels with the largest bedforms in particular, indicating a narrower range of applicability than methods using σ_z. For Manning's n prediction, none of the previously available methods performed well throughout the full range of measured flow resistance. The Jarrett (1984) equation predicted n with the lowest RMS error, but bias is apparent at higher resistance values ($n > \sim0.2$). This may be the result of lower slopes, bedform irregularity, and instream wood in the reaches used to develop the Jarrett dataset, in comparison with the Fraser dataset.

Relationships that rely solely upon the relative grain submergence, such as Bathurst (1985) and Lee and Ferguson (2002), performed poorly in the Fraser channels. The relatively poor performance of the Bathurst equation (Fig. 3c) was not surprising since it was developed for predicting grain resistance in lower-gradient channels, however the method also predicted poorly in a low-gradient, plane bed reach (ESL-6). This indicates that small-scale bed irregularities and bank form can substantially influence flow resistance. The Lee and Ferguson (2002) equation, which uses step grain size, was developed for streams in a similar slope range, using both field and laboratory data. However, these steps were entirely clast-formed. This is also the case in the dataset of Comiti
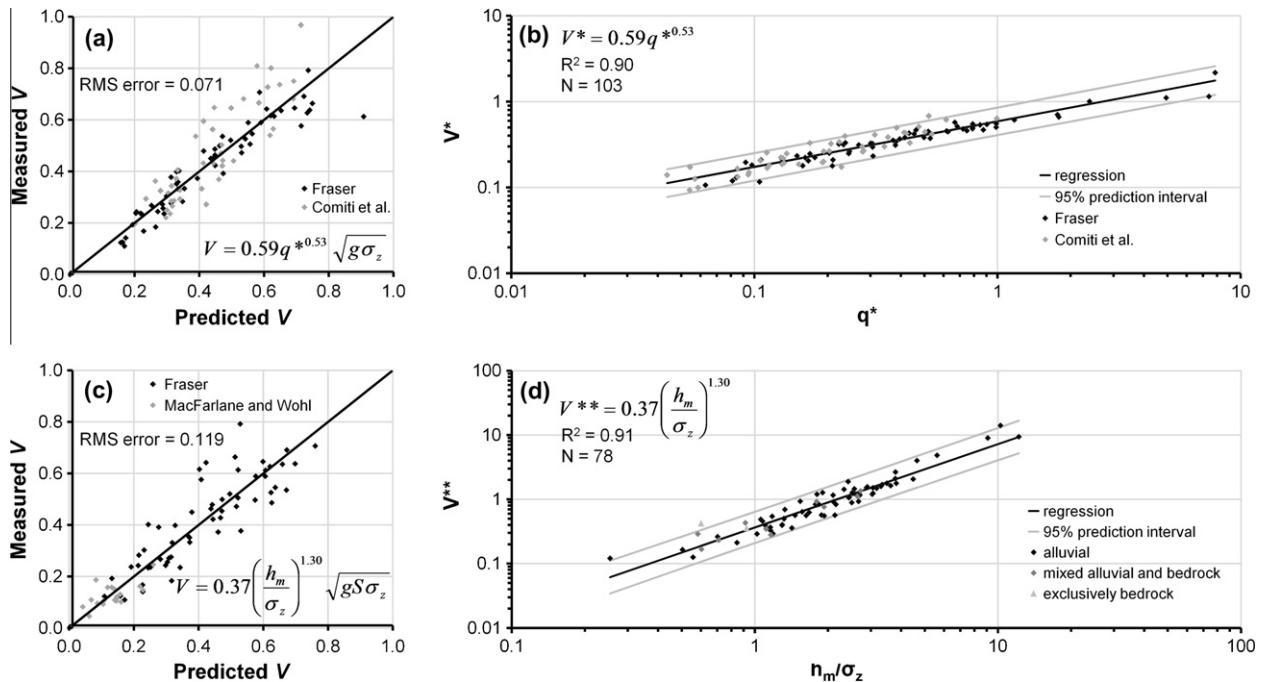
Fig. 6. Measured versus predicted performance and regressions for velocity using dimensionless discharge (with $D_c = \sigma_z$) and relative bedform submergence, based on the Fraser, MacFarlane and Wohl (2003) and Comiti et al. (2007) datasets. Ninety-five percent prediction intervals for the regressions are provided, with RMS error computed in normal space using only the Fraser database.
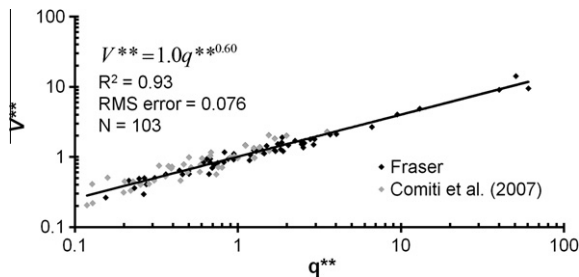
Fig. 7. Regression of V^{**} versus q^{**}, based on the Fraser and Comiti et al. (2007) datasets. RMS error is for the Fraser data.

et al. (2007), whose model consistently underpredicted resistance of the Fraser channels despite using a dimensionless velocity and discharge method (Eqs. (2) and (3)) that proved effective with their dataset. Similarly, direct velocity prediction methods performed poorly with the Fraser data, with RMS errors similar to or greater than the dataset average velocity of 0.44 m/s. These methods typically rely upon dimensionless velocity and unit discharge computed using D_{84} as the roughness parameter, D_c (Ferguson, 2007; Comiti et al., 2007; Comiti et al., 2009), with this method not accounting for instream wood increasing step heights and flow resistance. It has been found that substantial quantities of instream wood can increase flow resistance by up to an order of magnitude (Comiti et al., 2008), with the highest resistance channel having substantial spill resistance induced from wood steps.

The potential ramifications of overestimated velocity and underestimated resistance coefficients include underestimated travel times, the miscategorization of flow regime, inaccurate design parameters for hydraulic structures, and instability in computational modeling. The direct prediction of velocity has become popular (Ferguson, 2007; Comiti et al., 2007; Comiti et al., 2009; Zimmermann, 2010) despite a technical need for estimated resistance coefficients in such applications as computational modeling.

Furthermore, most recent prediction relationships have emphasized use of the Darcy-Weisbach equation over the Manning's equation (Lee and Ferguson, 2002; Aberle and Smart, 2003; Comiti et al., 2007). However, practicing professionals typically use Manning's n values when using resistance coefficients. This disconnection between application and published research is problematic for the community as a whole, with the problem compounded by the inadequate performance of existing relationships (Jarrett, 1984; Rickenmann, 1994) for n at higher resistances ($n > \sim 0.2$).

5.1. Models developed in this study

To satisfy the needs of practitioners who are called upon to predict velocity and flow resistance coefficients in high-gradient stream channels, methods are required to predict velocity directly, using discharge if it is available or only geometric characteristics if it is not, as well as through resistance coefficients, including Manning's n. Regression equations developed for the Fraser dataset indicate that relative bedform submergence is the best predictive variable examined for n and f, with up to 80% of the variance explained. To assess relevance beyond the Fraser channels, few datasets are compatible; the MacFarlane and Wohl (2003) and Curran and Wohl (2003) datasets are the most comparable. With the addition of the MacFarlane and Wohl (2003) dataset increasing the explained variance to 84% for f, it appears that the use of relative bedform submergence has potential for general application in streams both with and without step-forming instream wood, in high-gradient channels with beds of alluvium and a mixture of bedrock and alluvium. However, the subsequent decrease in explained variance to 73% with the addition of the Curran and Wohl (2003) dataset indicates that this method has less application in streams with substantial non-step instream wood present, though this decrease may also be explained by a reduction in the longitudinal profile point density.

For the direct prediction of velocity when discharge is known, high levels of explained variance and relatively low RMS error were obtained using models of both the form V^* vs. q^* and V^{**} vs. q^{**},

using the Fraser data alone as well as a database that includes Comiti et al. (2007) data (Fig. 6a and b). Predictions were made with RMS error as low as 0.071 (16% of the average velocity), in channels with substantial diversity in form, slope and discharge. The high explained variance of V^{**} vs. q^{**} ($R^2 = 0.97$) had slightly increased RMS error, indicating potential problems associated with use of common scaling variables in both dimensionless ratios. Given a known discharge, regression models from this combined dataset, with slopes ranging from 1.5% to 21% and discharge ranging from low through bankfull, predict the measured Fraser velocities with a surprising level of accuracy. Zimmermann (2010) found that there was no substantial advantage of the use of σ_z over D_{84} for velocity prediction using V^* vs. q^* in a laboratory channel without instream wood; however, there was also no disadvantage found. Ultimately, σ_z is no less effective than D_{84} for prediction in channels dominated by clast steps, but is much more effective than D_{84} in channels with instream wood heightening steps.

When discharge is unknown, an iterative approach may be effective for using dimensionless unit discharge for velocity prediction. Alternatively, relative bedform submergence can be used to predict velocity directly (Fig. 6c and d). This approach also avoids potential spurious self correlations problems associated with common scaling parameters in both explanatory and predicted variables. With the best model using h_m/σ_z providing RMS error of 0.11 m/s (25% of the average velocity), as compared to 0.071 m/s through the use of dimensionless discharge, predictions using this approach are not as accurate, though are still reasonable considering the complexity of the channels. Ferguson (2007) also found this to be the case and speculated that dimensionless unit discharge performs better than relative submergence for velocity prediction due to less sensitivity to measurement error and the computational effects of the large proportion of flow resistance being induced by form and spill, rather than grain, in step pool channels being canceled out with the use of dimensionless discharge, eliminating overall bias. Velocity is predicted with a slightly increased RMS error with the addition of the MacFarlane and Wohl (2003) dataset (model 23 and 24) while expanding the database further to include the Curran and Wohl (2003) dataset reduced the explained variance, illustrating the decrease in accuracy associated with a prevalence of non-step instream wood.

The scaling relation $V^{**} = q^{**0.6}$ developed in this study (model 20, Fig. 7) can be rearranged to give

$$\frac{V}{u^*} = \frac{h}{\sigma_z} \tag{8}$$

where $u^* = \sqrt{ghS_f}$, the shear velocity. With $D_c = \sigma_z$, and inclusion of the Darcy-Weisbach equation,

$$\frac{V}{u^*} = \sqrt{\frac{8}{f}} = \frac{h}{D_c} \tag{9}$$

This result is remarkably similar to the predictive equation of Aberle and Smart (2003) $V/u^* = 0.91 h/\sigma_z$ based on flume data, as well as the rational results of Rickenmann (1990; equation 5.20) and Nikora et al. (2001) for flow with small relative submergence. Eqs. (8) and (9) also support the roughness layer equation, as presented by Ferguson (2007). The high explanatory power of this relationship across both the flume data of Aberle and Smart (2003) and the field datasets examined in this study underscores the strong physical basis and transferability of this scaling relation.

Models 21 indicates that V is proportional to h/D_c. This is similar to previous findings that f is proportional to $(\delta/h)^2$, where h is larger than the roughness layer thickness, δ (Nikora et al., 2001). It has been hypothesized that this relationship is due to flow being heavily influenced by eddy creation (form resistance) in the wake

of roughness elements. (Nikora et al., 2001; Aberle and Smart, 2003). The composited dataset indicates that σ_z is analogous to the characteristic roughness layer thickness, as also asserted by Aberle and Smart, 2003. Additionally, analysis of low flow data (MacFarlane and Wohl, 2003) shows higher prediction errors with flow depths substantially less than σ_z, with situations where $\sigma_z \gg h_m$ resulting in substantially underestimated velocity.

5.2. Model caveats

An analysis of model residuals (of the Fraser data) indicates that resistance coefficient prediction using σ_z provides poorer predictions in channels with substantial non-step instream wood (Yochum, 2010), with densities greater than roughly 2–3% (by volume) substantially reducing the prediction accuracy. The two exclusively bedrock channels were variably predicted and the current evidence is insufficient to determine the appropriateness of the method in bedrock beds. Additionally, the Fraser residual analysis indicated that a single overall relationship predicted less effectively in lower-gradient channels with less pronounced bedforms and in the steepest channels at flows approaching bankfull. For both these situations, this may be due to shifts in regime, with the small bedforms in low gradient channels influencing velocity in a mechanistically different way than step pool and cascade channels, and a transition towards a skimming regime (Comiti et al., 2009) in high gradient channels. The multivariate regression analyses indicated that, beyond bedforms being the greatest contribution towards flow resistance (through form and spill resistance), the form resistance generated by bankforms is also a significant contributor. However, the relatively short length of some of the reaches may obscure the effect of bankforms in this analysis.

Most flow resistance is being developed in these channels by bedforms, through a combination of form and spill resistance (David et al., 2011), with relative bedform submergence and σ_z being effective descriptors of dominant resistance processes. It is convenient that a variable as relatively simple to measure in the field as σ_z (all that is needed is a single thalweg longitudinal profile) can explain such a high level of variance. This method has great potential for use in channels where bedforms are the primary source of flow resistance, with the Fraser and MacFarlane and Wohl datasets indicating strong predictive capabilities with $h_m > \sim 0.5\sigma_z$. A question that arises regarding the use of longitudinal profiles in quantifying bed variability is: what spacing is necessary to retain a high level of explained variance? With spacing described using a dimensionless channel width/spacing ratio, and an average ratio of 7.9 measured for the Fraser dataset, it was found that average point density could have been potentially reduced from an average width/spacing ratio of 7.9–4.1 with a small but detectable negative influence upon the predictions (Table 5) but reducing the ratio beyond this point resulted in substantially reduced predictive capabilities. The nature of the 25% reduction test involved creating non-uniform point spacing; these models being slightly weaker than the 50%-reduction test likely indicate the negative consequence of non-uniform point spacing. Ultimately, longitudinal profiles should be measured with uniform spacing at sufficient scale for quantifying bed variability.

Computational hydraulic modeling is a primary application of resistance coefficient estimation. Typically, modelers employ a constant Manning's n value throughout a full range of flows. This is inappropriate in high-gradient channels due to the substantial variability in resistance by stage. For example, in a Fraser reach (FC-4) n varied from 0.22 to 0.52 for bankfull through low flow. Other researchers have also noted that flow resistance in these channel types decreases with increasing stage (Lee and Ferguson, 2002; Reid and Hickin, 2008; Ferguson, 2010). If HEC-RAS or

another 1-dimensional model is applied to these stream types, the use of a constant n for a range of discharges would result in over- or under-estimated velocities at all but a single stage, at best. An advantage of n prediction based on relative bedform submergence is that it allows the application of the vertical variation in n values option that HEC-RAS provides. Such an approach is advisable in high-gradient channels.

5.3. Future research

Methods for predicting velocity using both discharge and geometric characteristics, as well as only geometric characteristics, are provided. Additionally, methods for estimating both Manning's n and Darcy-Weisbach f are presented. Error in the predictions is relatively low, especially considering the inherent complexity of

Table A1
Average reach velocity, flow resistance and geometric characteristics.

ID	Date	V (m/s)	Q (m³/s)	S_f (m/m)	L (m)	TW (m)	A (m²)	R (m)	h_m (m)	Fr#	n	f	σ_z	K_b	V_w/V_{H2O} (%)
ESL-1	2-August-07	0.28	0.11	0.091	31.4	2.0	0.29	0.12	0.25	0.24	0.25	10.4	0.19	1.24	–
	10-Junee-08	0.65	0.56	0.095	29.4	2.9	0.99	0.25	0.53	0.35	0.19	4.5	0.18	1.27	0.8
	22-July-08	0.42	0.24	0.105	27.3	2.6	0.70	0.20	0.44	0.26	0.27	9.4	0.21	1.21	0.6
ESL-2	9-July-07	0.45	0.22	0.093	13.9	2.9	0.68	0.20	0.40	0.30	0.23	7.0	0.16	1.47	3.5
	9-August-07	0.24	0.09	0.099	13.6	2.6	0.47	0.16	0.33	0.18	0.39	22.1	0.18	1.46	–
	6-June-08	0.61	0.53	0.094	13.7	3.2	1.00	0.25	0.49	0.35	0.20	4.8	0.19	1.30	3.4
	15-July-08	0.59	0.31	0.093	14.0	3.0	0.74	0.21	0.44	0.38	0.18	4.3	0.13	1.33	2.8
ESL-3	10-July-07	0.49	0.22	0.123	10.7	3.0	0.61	0.15	0.41	0.35	0.21	6.3	0.14	1.27	1.0
	9-August-07	0.38	0.09	0.119	11.3	2.4	0.42	0.14	0.38	0.29	0.25	9.2	0.14	1.32	–
	7-June-08	0.71	0.46	0.129	10.2	3.6	0.87	0.18	0.51	0.46	0.16	3.7	0.15	1.27	0.9
	15-July-08	0.54	0.30	0.119	10.7	3.5	0.80	0.17	0.49	0.36	0.20	5.7	0.16	1.18	0.7
ESL-4	10-July-07	0.45	0.21	0.123	15.8	2.5	0.57	0.18	0.35	0.30	0.25	8.7	0.20	1.43	0.1
	6-August-07	0.33	0.12	0.119	16.5	2.3	0.50	0.17	0.31	0.23	0.32	14.4	0.16	1.48	–
	7-June-08	0.63	0.61	0.120	15.6	2.9	0.99	0.26	0.50	0.34	0.23	6.3	0.18	1.42	0.5
	14-July-08	0.50	0.32	0.118	15.9	2.7	0.81	0.23	0.45	0.29	0.26	8.7	0.17	1.29	0.4
ESL-5	12-July-07	0.36	0.19	0.149	13.5	3.6	0.78	0.18	0.34	0.25	0.34	16.1	0.22	1.57	1.0
	8-August-07	0.27	0.10	0.134	15.1	3.3	0.59	0.15	0.29	0.20	0.38	21.8	0.22	1.52	–
	9-June-08	0.52	0.50	0.160	12.5	4.0	1.20	0.24	0.46	0.30	0.30	11.1	0.26	1.41	2.3
	14-July-08	0.48	0.33	0.143	13.9	4.0	1.09	0.22	0.42	0.29	0.29	10.8	0.24	1.38	2.3
ESL-6	13-July-07	0.58	0.19	0.015	6.5	2.7	0.56	0.19	0.25	0.40	0.07	0.7	0.03	1.07	0.3
	8-August-07	0.39	0.10	0.019	6.2	2.7	0.44	0.15	0.20	0.31	0.10	1.4	0.04	1.09	–
	9-June-08	1.32	0.52	0.024	6.4	3.0	0.89	0.26	0.38	0.77	0.05	0.3	0.04	1.07	0.4
	14-July-08	0.61	0.32	0.015	6.4	2.9	0.79	0.24	0.35	0.37	0.08	0.8	0.03	1.03	0.4
ESL-7	12-July-07	0.50	0.20	0.087	22.9	2.7	0.57	0.18	0.36	0.35	0.19	4.8	0.13	1.32	0.7
	4-August-07	0.40	0.10	0.082	24.3	2.5	0.42	0.15	0.31	0.31	0.20	6.0	0.15	1.38	–
	8-June-08	0.69	0.52	0.085	22.1	3.0	0.97	0.25	0.49	0.39	0.17	3.5	0.14	1.27	0.7
	15-July-08	0.55	0.30	0.081	24.0	2.9	0.86	0.23	0.46	0.32	0.19	4.8	0.12	1.26	0.7
ESL-8	11-July-07	0.46	0.21	0.089	31.4	2.7	0.59	0.18	0.38	0.32	0.21	6.0	0.15	1.41	0.3
	5-August-07	0.35	0.10	0.081	35.5	2.6	0.48	0.16	0.32	0.26	0.24	8.2	0.13	1.49	–
	9-June-08	0.64	0.46	0.094	30.7	3.2	0.91	0.23	0.49	0.38	0.18	4.2	0.14	1.39	0.6
	16-July-08	0.53	0.29	0.087	32.6	3.0	0.78	0.21	0.44	0.33	0.20	5.3	0.12	1.42	0.4
ESL-9	11-July-07	0.43	0.20	0.103	16.2	2.6	0.65	0.20	0.39	0.27	0.26	8.8	0.16	1.41	0.7
	6-August-07	0.33	0.11	0.090	18.6	2.3	0.47	0.17	0.33	0.23	0.28	10.9	0.18	1.39	–
	8-June-08	0.64	0.57	0.115	16.3	2.8	0.92	0.25	0.52	0.36	0.21	5.5	0.16	1.33	1.2
	16-July-08	0.47	0.28	0.097	16.5	2.6	0.72	0.22	0.44	0.29	0.24	7.4	0.16	1.26	0.6
FC-1	5-July-07	0.40	0.049	0.061	23.7	1.6	0.18	0.10	0.18	0.38	0.13	3.0	0.08	1.15	0.2
	12-August-07	0.19	0.014	0.057	25.1	1.3	0.09	0.06	0.12	0.23	0.20	7.6	0.08	1.16	–
	11-June-08	0.79	0.233	0.063	23.1	2.0	0.38	0.16	0.29	0.58	0.09	1.3	0.06	1.07	0.4
	23-July-08	0.30	0.037	0.061	23.2	1.6	0.17	0.10	0.17	0.29	0.17	5.0	0.07	1.12	0.2
FC-2	7-July-07	0.37	0.043	0.072	15.1	1.4	0.17	0.10	0.21	0.34	0.16	4.1	0.05	1.25	1.8
	12-August-07	0.17	0.013	0.068	14.9	1.1	0.08	0.06	0.13	0.20	0.24	11.4	0.05	1.23	–
	11-June-08	0.66	0.243	0.071	14.4	1.6	0.39	0.18	0.34	0.44	0.13	2.2	0.09	1.18	1.1
	23-July-08	0.28	0.038	0.072	14.2	1.4	0.20	0.11	0.22	0.24	0.22	8.0	0.08	1.19	1.5
FC-3	6-July-07	0.26	0.045	0.089	14.9	1.6	0.23	0.11	0.23	0.22	0.27	11.8	0.11	1.31	3.4
	11-August-07	0.12	0.013	0.087	14.9	1.4	0.12	0.07	0.14	0.13	0.41	31.4	0.11	1.40	–
	12-June-08	0.51	0.216	0.092	13.5	2.1	0.55	0.19	0.38	0.32	0.20	5.4	0.12	1.24	4.3
	22-July-08	0.18	0.039	0.099	12.2	1.7	0.24	0.11	0.23	0.15	0.40	26.3	0.11	1.46	4.2
FC-4	7-July-07	0.24	0.042	0.132	19.0	1.4	0.23	0.12	0.24	0.20	0.36	21.1	0.15	1.33	0.6
	11-August-07	0.14	0.014	0.132	19.2	1.2	0.14	0.09	0.17	0.13	0.52	46.9	0.12	1.31	–
	12-June-08	0.59	0.216	0.135	18.9	1.6	0.48	0.21	0.43	0.34	0.22	6.3	0.17	1.19	1.7
	21-July-08	0.27	0.045	0.127	19.8	1.4	0.21	0.12	0.25	0.22	0.31	15.8	0.15	1.27	1.0
FC-5	8-July-07	0.24	0.015	0.171	13.1	0.9	0.09	0.08	0.15	0.24	0.31	18.2	0.10	1.25	0.1
	10-August-07	0.11	0.007	0.157	14.2	0.8	0.05	0.05	0.11	0.13	0.52	55.6	0.09	1.25	–
	25-June-08	0.64	0.147	0.186	11.9	1.1	0.20	0.13	0.26	0.49	0.17	4.5	0.14	1.08	0.2
	17-July-08	0.24	0.017	0.184	11.9	0.9	0.10	0.08	0.17	0.24	0.32	18.9	0.16	1.16	0.1
FC-6	8-July-07	0.24	0.014	0.184	19.8	0.9	0.08	0.07	0.14	0.25	0.31	17.8	0.13	1.27	0.4
	10-August-07	0.12	0.007	0.165	22.1	0.7	0.04	0.05	0.10	0.15	0.44	41.9	0.14	1.32	–
	25-June-08	0.62	0.141	0.200	19.1	1.1	0.17	0.12	0.24	0.50	0.17	4.8	0.13	1.20	0.5
	17-July-08	0.23	0.017	0.178	20.6	0.9	0.09	0.07	0.17	0.24	0.32	18.9	0.13	1.27	0.5

high-gradient channels. Despite the strong performance of these methods, other sources of flow resistance also contribute to the overall resistance than the bedforms primarily quantified using these methods. Bank variability has also been found to be significant, but a more comprehensive analysis of bank variability impact on flow resistance is warranted. Additionally, the Curran and Wohl (2003) dataset indicate that the influence of non-step instream wood can substantially increase flow resistance. Methods quantifying the increase in form resistance induced by instream wood, such as the approach presented in Kaufmann et al. (2008), could enhance predictions. Additionally, the Fraser data indicate a potential regime shift at higher gradients and discharges, into a transitional/skimming regime (Comiti et al., 2009). This deserves additional evaluation. While velocity in both alluvial and mixed alluvial-bedrock channels was predicted with reasonable accuracy (Fig. 6d), the two bedrock measurements do not provide sufficient information to draw conclusions regarding method effectiveness in this bed type. The collection of additional data in high-gradient bedrock channels would be helpful to judge the merits of this methodology in this channel type. Finally, consideration of these results combined with the previous finding that σ_z can have predictive capabilities in sand bed channels with dune bedforms (Aberle et al., 2010) indicate that this approach may have merit in other channels where bedforms substantially contribute to flow resistance, such as pool-riffle and dune-ripple streams.

6. Conclusions

The ability to effectively predict velocity and flow resistance coefficients is essential for numerous practical applications including hydraulic modeling, stream restoration design, geomorphic analysis, and ecological studies. A database of 59 field-collected measurements of reach-average velocity and flow resistance was assembled for 15 reaches with substantial step-forming instream wood present. These data were combined with field data collected by other researchers in streams both with and without wood, in alluvial and mixed alluvial-bedrock channels. Through the evaluation of both existing and modified methodologies, we found that resistance coefficients and velocity prediction techniques that are based upon grain size and relative grain submergence performed poorly, including dimensionless methods with $D_c = D_{84}$. This is due to particle size based prediction ignoring bedforms induced by material other than grains, such as step height enhancement by instream wood. Methods for velocity and resistance coefficient prediction based upon the standard deviation of bed elevations, σ_z, and relative bedform submergence, h/σ_z, substantially improve prediction accuracy in the tested channels. The most accurate approach for predicting velocity was through the use of dimensionless variables, with the characteristic roughness parameter $D_c = \sigma_z$ to account for step height enhancement by wood. Where discharge is unknown, h/σ_z performed well for the direct prediction of velocity. Additionally, an empirical relationship was rearranged to give $V/u^* = h/\sigma_z$, providing a rigorous test of previously-derived results using field based data collected in complex mountain stream channels. Using these field data, guidance was provided regarding the minimum depth limit of applicability and maximum point longitudinal spacing required to sufficiently capture bed variability. A key advantage of the use of σ_z is that it captures the influence of the largest clasts in forming steps, the combined influence of clasts and instream wood in heightening steps, and the variability in bedrock beds. Hence, σ_z is indicated to be the most appropriate roughness parameter for predicting flow resistance and velocity in high-gradient channels. Additionally, if a quasi-natural step-pool form is applied to engineered channels, similar approaches may be applicable in the design of structures for rehabilitating or stabilizing high-gradient channels.

Appendix A

See Table A1.

References

Aberle, J., Smart, G.M., 2003. The influence of roughness structure on flow resistance on steep slopes. J. Hydraul. Res. 41 (3), 259–269.

Aberle, J., Nikora, V., Henning, M., Ettmer, B., Hentschel, B., 2010. Statistical characterization of bed roughness due to bed forms: a field study in the Elbe River at Aken, Germany. Water Resour. Res. 46, W03521. doi:10.1029/2008WR007406.

Abt, S.R., Wittier, R.J., Ruff, J.K., Khattak, M.S., 1988. Resistance to flow over riprap in steep channels. Water Resour. Bull. 24 (6), 1193–1200.

Arcement, G.J., Schneider, V.R., 1989. Guide for Selecting Manning's Roughness Coefficients for Natural Channels and Flood Plains. US Geological Survey Water-Supply Paper 2339.

Ataman, E., Aatre, V.K., Wong, K.M., 1981. Some statistical properties of median filters. IEEE Trans. Acoust. Speech Signal Process. 29 (5), 1073–1075.

Bathurst, J.C., 1985. Flow resistance estimation in mountain rivers. J. Hydraul. Eng. 111 (4), 625–643.

Brunner, G.W., 2010. HEC-RAS River Analysis System Hydraulic Reference Manual. Report CPD-69. US Army Corps of Engineers, Hydrologic Engineering Center.

Chin, A., Phillips, J.D., 2007. The self-organization of step-pools in mountain streams. Geomorphology 83, 346–358.

Chow, V.T., 1959. Open Channel Hydraulics. McGraw-Hill Book Company, New York.

Comiti, F., Andreoli, A., Mao, L., Lenzi, M.A., 2008. Wood storage in three mountain streams of the Southern Andes and its hydro-morphological effects. Earth Surface Process. Land. 33, 244–262.

Comiti, F., Cadol, D., Wohl, E., 2009. Flow regimes, bed morphology, and flow resistance in self-formed step-pool channels. Water Resour. Res. 45, W04424. doi:10.1029/2008WR007259.

Comiti, F., Mao, L., Wilcox, A., Wohl, E.E., Lenzi, M.A., 2007. Field-derived relationships for flow velocity and resistance in high-gradient streams. J. Hydrol. 340, 48–62.

Curran, J.H., 1999. Hydraulics of Large Woody Debris in Step-Pool Channels, Cascade Range, Washington. Masters Thesis, Colorado State University, Fort Collins, CO, USA.

Curran, J.H., Wohl, E.E., 2003. Large woody debris and flow resistance in step-pool channels, Cascade Range, Washington. Geomorphology 51 (1–3), 141–157.

David, G.C.L., Wohl, E., Yochum, S.E., Bledsoe, B.P., 2010a. Controls on spatial variations in flow resistance along steep mountain streams. Water Resour. Res. 46, W03513. doi:10.1029/2009WR008134.

David, G.C.L., Wohl, E., Yochum, S.E., Bledsoe, B.P., 2010b. Controls on at-a-station hydraulic geometry in steep headwater streams, Colorado, USA. Earth Surface Processes and Landforms 35, 1820–1837.

David, G.C.L., Wohl, E., Yochum, S.E., Bledsoe, B.P., 2011. Comparative analysis of bed resistance partitioning in high gradient streams. Water Resour. Res. doi:10.1029/2010WR009540.

Ferguson, R., 2007. Flow resistance equations for gravel- and boulder-bed streams. Water Resour. Res. 43, W05427. doi:10.1029/2006WR005422.

Ferguson, R., 2010. Time to abandon the manning equation? Earth Surface Process. Land. 35, 1873–1876. doi:10.1002/esp. 2091.

Gallagher, N.C., Wise, G.L., 1981. A theoretical analysis of the properties of median filters. IEEE Trans. Acoust. Speech Signal Process. 29 (6), 1136–1141.

Hassan, M.A., Reid, I., 1990. The influence of microform bed roughness elements on flow and sediment transport in gravel bed rivers. Earth Surface Process. Land. 15, 739–750. doi:10.1002/esp. 3290150807.

Jarrett, R.D., 1984. Hydraulics of high-gradient streams. J. Hydraul. Eng. 110 (11), 1519–1539.

Kaufmann, P.R., 1987. Channel Morphology and Hydraulic Characteristics of Torrent-Impacted Forest Streams in the Oregon Coast Range, USA. PhD Dissertation, Oregon State University, Corvallis, OR, USA.

Kaufmann, P.R., Faustini, J.M., Larsen, D.P., Shirazi, M.A., 2008. A roughness-corrected index of relative bed stability for regional stream surveys. Geomorphology 99, 150–170.

Koll, K., 2002. Feststofftransport und Geschwindigkeitsverteilung in Raugerinnen Diss. Univ. Karlsruhe, Fak. f. Bauingenieur, und Vermessungswesen.

Lee, A.J., Ferguson, R.I., 2002. Velocity and flow resistance in step-pool streams. Geomorphology 46, 59–71.

Limerinos, J.T., 1970. Determination of the Manning Coefficient from Measured Bed Roughness in Natural Channels. US Geological Survey Water-Supply Paper 1898-B.

MacFarlane, W.A., Wohl, E., 2003. Influence of step composition on step geometry and flow resistance in step-pool streams of the Washington Cascades. Water Resour. Res. 39(2), 1037. doi:10.1029/2001WR001238.

Montgomery, D.R., Buffington, J.M., 1997. Channel reach morphology in mountain drainage basins. Geol. Soc. Am. Bull. 109 (5), 596–611.

Mussetter, R.A., 1988. Dynamics of Mountain Streams. PhD Dissertation, Colorado State University, Fort Collins, Colorado.

Nikora, V., Goring, D., McEwan, I., Griffiths, G., 2001. Spatially averaged open-channel flow over rough bed. J. Hydraul. Eng. 127 (2), 123–133.

Pagliara, S., Chiavaccini, P., 2006. Flow resistance of rock chutes with protruding boulders. J. Hydraul. Eng. 132 (6), 545–552.

Parker, G., Wilcock, P.R., Paola, C., Dietrich, W.E., Pitlick, J., 2007. Physical basis for quasi-universal relations describing bankfull hydraulic geometry of single-thread gravel bed rivers. J. Geophys. Res. 112, F04005. doi:10.1029/2006JF000549.

Reid, D.E., Hickin, E.J., 2008. Flow resistance in steep mountain streams. Earth Surface Process. Land. 33, 2211–2240.

Rice, C.E., Kadavy, K.C., Robinson, K.M., 1998. Roughness of loose rock riprap on steep slopes. J. Hydraul. Eng. 124 (2), 179–185.

Rickenmann, D., 1994. An alternative equation for the mean velocity in gravel-bed rivers and mountain torrents. In: Cotroneo, G.V., Rumer, R.R. (Eds.), Hydraulic Engineering '94, Proceedings of the 1994 Conference, vol. 1. ASCE, New York.

Rickenmann, D., Recking, A., 2011. Evaluation of flow resistance equations using a large field data base. Water Resour. Res. doi:10.1029/2010WR009793.

Rosport, M., 1997. Fließwiderstand und Sohlstabilität steiler Fließgewässer unter Berücksichtigung gebirgsbachtypischer Sohlstrukturen, Mitt. des Instituts für Wasserwirtschaft und Kulturtechnik, Univ. Karlsruhe Heft 196.

Rouse, H., 1965. Critical analysis of open-channel resistance. ASCE J. Hydraul. Div. 91, 1–25.

Thompson, S.M., Campbell, S.M., 1979. Hydraulics of a large channel paved with boulders. J. Hydraul. Res. 17, 341–354.

Tukey, J.W., 1974. Nonlinear (nonsuperposable) methods for smoothing data. IEEE Electron. Aerosp. Syst. Conv. 673.

Walden, M.G., 2004. Estimation of average stream velocity. J. Hydraul. Eng. 130 (11), 1119–1122.

Wilcox, A.C., Wohl, E.E., 2006. Flow resistance dynamics in step-pool stream channels: 1. Large woody debris and controls on total resistance. Water Resour. Res. 42, W05418. doi:10.1029/2005WR004277.

Wilcox, A.C., Nelson, J.M., Wohl, E.E., 2006. Flow resistance dynamics in step-pool stream channels: 2. Partitioning between grain, spill and woody debris resistance. Water Resour. Res. 42, W05419. doi:10.1029/2005WR004278.

Wohl, E., Madsen, S., MacDonald, L., 1997. Characteristics of log and clast bed-steps in step-pool streams of northwestern Montana, USA. Geomorphology 20, 1–10.

Wohl, E., Merritt, D.M., 2008. Reach-scale channel geometry of mountain streams. Geomorphology 93, 168–185.

Yochum, S.E., 2010. Flow Resistance Prediction in High-Gradient Streams. PhD Dissertation, Colorado State University, Fort Collins, CO, USA.

Yochum, S., Bledsoe, B., 2010. Flow resistance estimation in high-gradient streams. In: 4th Federal Interagency Hydrologic Modeling Conference, June 27–July 1, Las Vegas, Nevada, USA.

Zimmermann, A., 2010. Flow resistance in steep streams: an experimental study. Water Resour. Res. 46, W09536. doi:10.1029/2009WR007913.